The ac Josephson relation and inhomogeneous temperature distributions in large $Bi_2Sr_2CaCu_2O_{8+\delta}$ mesas for THz emission

2013 Supercond. Sci. Technol. 26 085016

(http://iopscience.iop.org/0953-2048/26/8/085016)

Supercond. Sci. Technol. **26** (2013) 085016 (6pp) doi:10.1088/0953-2048/26/8/085016

The ac Josephson relation and inhomogeneous temperature distributions in large $Bi_2Sr_2CaCu_2O_{8+\delta}$ mesas for THz emission

T M Benseman[1], A E Koshelev[1], W-K Kwok[1], U Welp[1], K Kadowaki[2], J R Cooper[3] and G Balakrishnan[4]

[1] Materials Science Division, Argonne National Laboratory, Argonne, IL 60439, USA
[2] Institute for Materials Science, University of Tsukuba, Ibaraki 305-8753, Japan
[3] Cavendish Laboratory, University of Cambridge, Cambridge CB3 0HE, UK
[4] Department of Physics, University of Warwick, Coventry CV4 7AL, UK

E-mail: tbenseman@anl.gov

Received 11 May 2013, in final form 11 June 2013
Published 1 July 2013
Online at stacks.iop.org/SUST/26/085016

Abstract
We have studied the terahertz emission from a 720 × 60 × 1.2 μm^3 mesa patterned from under-doped $Bi_2Sr_2CaCu_2O_{8+\delta}$. This device has an S-shaped current–voltage characteristic due to self-heating, allowing us to compare its THz emission behaviours at up to three different bias currents for the same voltage. The THz frequency generated along the lowest current branch follows the expected Josephson relation for a stack of intrinsic Josephson junctions connected in series. However, in the high current regimes, THz emission occurs at a significantly lower frequency than expected. We show that this behaviour is consistent with strongly non-uniform self-heating of the mesa at high bias currents.

(Some figures may appear in colour only in the online journal)

The observation [1] of the emission of coherent, continuous-wave THz-radiation from stacks of intrinsic Josephson junctions (IJJs) [2] in the layered high-T_c superconductor $Bi_2Sr_2CaCu_2O_{8+\delta}$ (Bi-2212) has generated considerable interest in the collective dynamics of large IJJ arrays [3–14]. The relatively large values of the off-chip radiation powers of tens of microwatts [11, 14] indicate that a substantial fraction of the IJJs in the stack are synchronized and emit coherently. The observed emission frequencies range from ∼0.4 to ∼1 THz and are found to scale inversely with the width of the junction stacks [1, 8, 11] suggesting that an electromagnetic cavity resonance promotes the synchronization of the junctions [15]. Junction stacks for THz emission have typical sizes of ∼1–2 μm height, corresponding to roughly 1000 IJJs, and lateral dimensions ∼50–100 μm in width and several 100 μm in length. Extensive work [16] has established that such stacks of IJJs are prone to strong self-heating effects most clearly evidenced by the pronounced S-shape of their current–voltage characteristics. Two regimes of THz emission from IJJ-stacks have been identified: the low-bias regime where self-heating effects can be neglected and the temperature in the stack is essentially uniform and close to the cryostat temperature, and the high-bias regime where self-heating causes strongly non-uniform temperature distributions inside the stack. Low temperature scanning laser microscopy (LTSLM) [5, 7, 9], thermal imaging [14, 17] as well as solutions to the heat diffusion equation [18, 19] reveal hot spots in which the temperature can exceed T_c and that are accompanied by large lateral temperature gradients. Nonetheless, it has been shown that in the low as well as in the high-bias regimes the ac Josephson relation in terms of the voltage applied across the stack is fulfilled [9, 11, 13]. This implies that the voltage per junction and the temperature distribution are uniform along the thickness of the stack.

Here we present results on c-axis transport and THz emission on a 60 × 720 μm^2 mesa patterned onto a slightly under-doped Bi-2212 crystal. Polycrystalline phase-pure

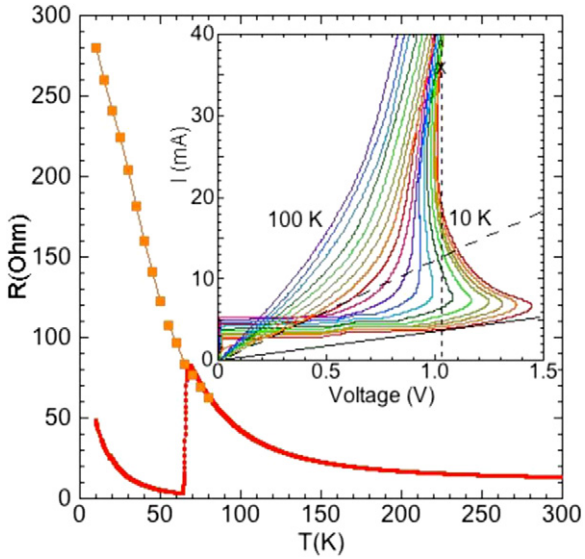

Figure 1. Temperature dependence of the *c*-axis resistivity measured directly at a low current of 10 μA (red symbols) and estimated from the sub-gap voltage as indicated by the solid line in the inset (orange squares). The inset shows the return branches of *I*–*V* curves measured at temperatures between 10 and 100 K every 5 K. The dashed line indicates a resistance of 83 Ω, the resistance at T_c. The cross marks the bias point at 36.55 mA and 15 K at which a clear emission line is seen (see figure 2), even though the average mesa temperature is substantially above T_c.

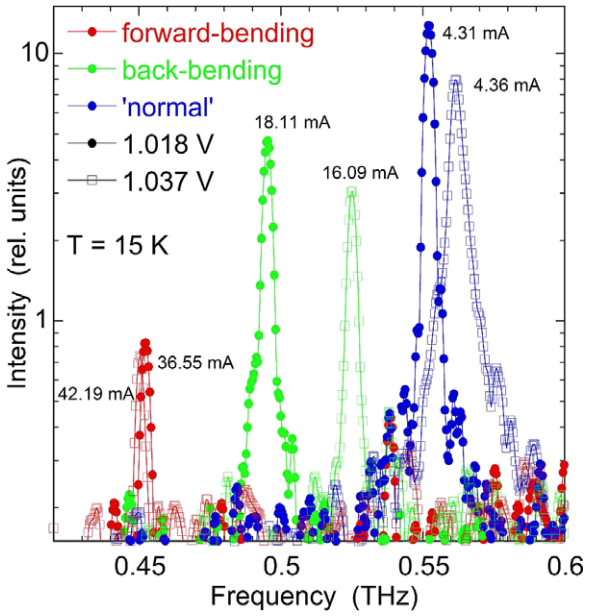

Figure 2. FTIR emission spectra at 15 K taken at mesa voltages of 1.018 V (closed circles) and 1.037 V (open squares) in the 'normal' (blue), back-bending (green) and forward-bending (red) regions. The bias current corresponding to each emission line is indicated.

Bi-2212 powder was prepared in Cambridge, and single crystals were grown at the University of Warwick by the travelling solvent floating zone method [20, 21]. At Argonne mesa devices were patterned on the surface of the crystal using photolithography and Ar-ion milling. The height of the mesa is ∼1.2 μm. The emission frequency in the high-bias regime shows unexpected re-entrant behaviour and deviation from the ac Josephson relation in terms of applied voltage indicating that temperature gradients in the vertical direction are important. Our results can be explained in a model in which the stack is composed of colder layers near its bottom and hot layers near its top. This model also accounts for the observation that emission persists up to bias currents at which the average stack temperature exceeds T_c by a factor of two.

Figure 1 shows the temperature dependence of the *c*-axis resistance of the IJJ stack measured with a current of 10 μA. The monotonic increase of the resistance with decreasing temperature, as well as the value of $T_c \sim 65$ K are indicative of the under-doped nature of the material. Below the superconducting transition the resistance again increases with further decreasing temperature, which we attribute to non-superconducting junctions at the top of the mesa. The inset of figure 1 shows the return branches of the current–voltage characteristics measured at various temperatures between 10 and 100 K. Here, the voltage values have been corrected for a contact resistance of 3.3 Ω, corresponding to the value of R_c just below T_c; see the appendix for a detailed discussion of the contact resistance. The pronounced back-bending of the *I*–*V* curves is a manifestation of significant self-heating as has been described extensively before for large mesas [16, 18, 19]. At temperatures below 45 K we can distinguish three regimes: the 'normal' regime at the bottom of the *I*–*V* curves, the back-bending regime at intermediate bias currents characterized by $\partial I/\partial V < 0$, and the forward-bending regime at very high current bias with $\partial I/\partial V > 0$. A feature typically not seen in *I*–*V* curves of such large mesas is the fact that re-switching of the junctions to the zero-resistance state occurs at relatively low voltages such that the return branch approaches a linear curve through the origin (solid line in figure 1) enabling the estimation of the *c*-axis resistance at temperatures below T_c from the sub-gap resistance. The results, included in the main panel of figure 1 as orange squares, reveal that at low temperatures the *c*-axis resistance saturates and increases approximately linearly with decreasing temperature [22] at a rate of ∼3.8 Ω K^{-1}.

Owing to the S-shape of the *I*–*V* curves there are—in principle—up to three working points for a given mesa voltage at which THz emission can occur [23]. This is indeed the case as shown in the FTIR spectra (figure 2) taken at 15 K and bias voltages of 1.018 and 1.037 V. Three sets of emission lines at different frequencies and corresponding to the 'normal', back-bending and forward-bending regimes, respectively, are clearly resolved. The emission lines near 0.57 THz are in good agreement with previous results on 60 μm wide mesas [1].

The evolution of the emission frequency with bias voltage and temperature is summarized in figure 3(a). The corrections for the contact resistance are described in detail in the appendix. The linear dependence in the 'normal' regime (top left) is expected on the basis of the ac Josephson relation [9, 11, 13], which—in the units of figure 3(a)—reads $f = 482.7\ (\text{THz V}^{-1})V_{\text{jct}}$. In the 'normal' regime self-heating can be neglected, and the mesa can be considered as a uniform

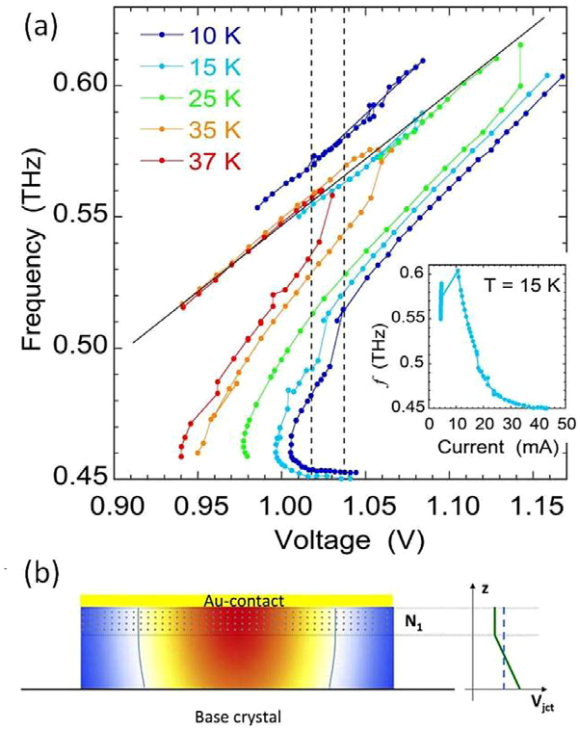

Figure 3. (a) Summary of the voltage dependence of the emission frequencies. The vertical dotted lines indicate the location of the spectra shown in figure 2. The solid line represents the Josephson relation. The inset shows the dependence of the emission frequency on bias current at 15 K. (b) Schematic showing the temperature distribution and synchronized junctions (shown dotted) in a mesa. The curved vertical lines indicate the $T = T_c$ boundaries. In the back-bending region, the N_1 synchronized junctions have constant junction voltage whereas for the unsynchronized junctions the junction voltage increases such that the total mesa voltage is the same as in the 'normal' region (blue dashed line).

system. Then the junction voltage V_{jct} is related to the mesa voltage V through $V_{jct} = V/N$, where N is the number of junctions in the mesa. Thus, the slope of the frequency data of ~0.53 THz V^{-1} implies a junction number of $N \sim 920$, in good agreement with the physical size of the sample. The frequency data at 10 K follow a linear dependence with slightly higher slope corresponding to about 2% fewer emitting junctions.

In the back-bending and forward-bending regions the emission frequency does not follow the Josephson relation as function of mesa voltage. This is a manifestation of the fact that the mesa voltage is no longer related in a simple way to the junction voltage, since the system has become inhomogeneous. LTSLM [5, 7, 9], thermal imaging [14, 17] as well as numerical solutions of the heat diffusion equation [18, 19] indicate a strongly non-uniform lateral temperature distribution under bias conditions corresponding to the back-bending and forward-bending regimes. The strong temperature dependence of the *c*-axis resistivity can cause an electro-thermal instability accompanied by the formation of hot spots that are characterized by a strongly enhanced temperature and current density as compared to the rest of the mesa. Nevertheless, due to the very large anisotropy of the in-plane and out-of-plane resistivities of BSCCO we can consider the *ab*-planes as equipotentials. Thus, even in the presence of large in-plane temperature gradients the voltage per junction would be uniform along the *c*-axis, and the Josephson relation in terms of the mesa voltage would apply. This has been observed in previous reports [9, 11, 13]. In contrast, the data in figure 3(a) indicate non-uniformity along the *c*-axis.

The mere fact that we observe THz emission at reasonably high power in the back-bending region implies that a large fraction of the junctions in the mesa are synchronized. The voltage per junction in this group of synchronized junctions is reduced with respect to emission in the 'normal' region by the ratio of emission frequency for the same mesa voltage. For example, at 1.037 V across the mesa the emission frequency, and therefore the junction voltage of the emitting junctions, is reduced by a factor of $k_1 = 0.93$. Generally, one finds that in the 'normal' region the voltage across the stack is given as $V_0 = NV_{jct,0} = NI_0 r_{jct,0}$ whereas in the back-bending regime it is $V_1 = N_1 V_{jct,1} + (N - N_1) I_1 \bar{r} = N_1 I_1 r_{jct,1} + (N - N_1) I_1 \bar{r}$ (see figure 3(b)). Here, $V_{jct,0}$ and $V_{jct,1}$ are the junction voltages at bias currents I_0 and I_1 in the 'normal' region and of the N_1 emitting junctions in the back-bending region, respectively, and $\bar{r}$ is the average junction resistance of the $(N - N_1)$ remaining non-emitting junctions. N_1 is not known *a priori*; however, the evolution of the emission power in the 'normal', back-bending and forward-bending regions (see figure 4) suggests that a sizeable fraction of the junctions does not emit. The reduction in emission frequency by a factor of k implies $V_{jct,1} = k_1 V_{jct,0}$ i.e., $r_{jct,1} = k_1 \frac{I_0}{I_1} r_{jct,0}$. For the 1.037 V data in figure 2 this yields a reduction of the junction resistance of the emitting junctions in the back-bending regime by a factor of four. Considering the temperature dependence of R_c displayed in figure 1 this reduction would imply an increase in average temperature from 15 to ~80 K, that is, above T_c. A similar analysis for the emission in the forward-bending regime yields $k_2 = 0.81$ and a reduction of the resistance of the emitting junctions by 1/12, corresponding to an average junction temperature of ~155 K, consistent with the notion that in the back-bending and forward-bending regions the lateral temperature distribution is very inhomogeneous, consisting of hot spots with temperature above T_c and cold regions (near the ends of the stack) that are still superconducting, see figure 2(b) in [18]. The large length/width aspect ratio of the mesa studied here—namely 12—promotes this appearance of a largely normal conducting core of the mesa with the ends of the mesa still being superconducting. Since the *ab*-planes are equipotentials, the junction resistance, junction voltage and emission frequency are determined by the normal conducting short in the hot spot. Furthermore, with $V_0 = V_{1,2}$, it follows that $\frac{\bar{r}}{r_{jct,1,2}} = \frac{1/k - n_{1,2}}{1 - n_{1,2}} \geq 1$ with $n_{1,2} = N_{1,2}/N$. The average resistance of the unsynchronized junctions is larger than that of the synchronized junctions implying that the average temperature of the synchronized junctions is higher than the average of the remainder of the stack. Since cooling occurs predominantly through the base crystal, our results suggest that the emission originates from junctions located near the

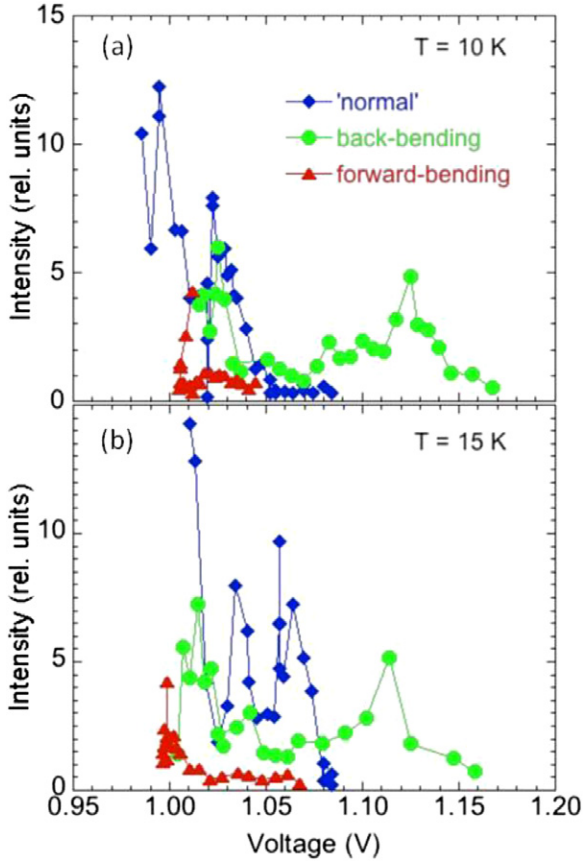

Figure 4. Voltage dependence at 10 K (a) and 15 K (b) of the emission intensity in the 'normal', back-bending and forward-bending regions.

ends of the mesa and near its top (see figure 3(b)). A location near the top electrode would be consistent with the mode profile of the resonant cavity mode, which has a maximum at the top electrode and a node near the interface with the base crystal [10].

As the mesa enters the forward-bending region the emission frequency displays an unusual re-entrant behaviour as function of mesa voltage. We note though that as a function of increasing bias current the emission frequency monotonically decreases (see inset of figure 3). We attribute these features to the interplay of two opposite trends: (a) with increasing bias current self-heating increases, and, as ρ_c is a monotonically decreasing function of temperature, the junction resistance $r_{jct}[T(I)]$ decreases; (b) the quasi-particle voltage $r_{jct}[T(I)]I$ may increase or decrease depending on the magnitude of $\partial\rho_c/\partial T$. Since the I–V curve in the region of emission is almost vertical, this interplay will depend sensitively on the details of the temperature distribution in the mesa. Furthermore, cooling through the gold contact, even though generally considered much weaker than cooling through the base crystal [18], may affect the temperature balance as well. We expect though that as the mesa has fully made the transition into the forward-bending region, the emission frequency would increase again with mesa voltage.

The voltage dependence of the frequency at 10 and 15 K displays a step near 0.5 THz. The origin of these steps has not been established yet; however, as shown in figure 5, the

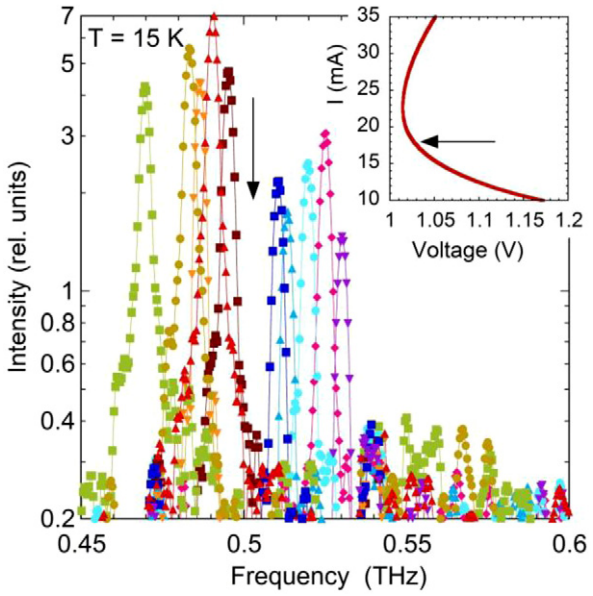

Figure 5. Evolution of the emission lines at 15 K in the vicinity of the step in frequency as seen in figure 3. The vertical arrow marks the location of the step. The inset shows a close-up of the I–V curve around the bias point of 18 mA corresponding to the step.

emission line shape changes systematically when going across the step, the location of which is indicated by the vertical arrow. At lower frequencies—i.e., higher bias current—the lines develop shoulders at low intensities. This may indicate the excitation of additional modes, which could arise for example when the hot core completely separates the two ends. There are though no discernable features in the I–V curve at the bias current of 18 mA corresponding to the step such as jumps that might indicate the motion of a hot spot, for instance [5, 9].

In summary, we have shown that Bi-2212 mesas can emit in two or even three distinct current regimes at certain mesa voltages, given the correct device dimensions and doping state of the material. This allows the properties of 'low-bias' and 'high-bias' THz emission regimes to be directly compared for the same mesa device. We find that while the emission frequency of the lowest current branch obeys the expected Josephson relation for a stack containing N IJJs, the observed THz frequency becomes significantly lower than this in the high current regime(s). While this behaviour may at first seem counterintuitive, it is consistent with the stack becoming thermally inhomogeneous due to high DC power dissipation. As a hot spot shorts the junctions most effectively at the top of the stack, a subset of phase-locked junctions forms there, having $V_{jct} < V_{mesa}/N$ and thus a lower-than-expected Josephson frequency. This phenomenon must be taken into consideration when designing Bi-2212 mesa devices for emission in the high-bias regime.

Acknowledgments

Work at Argonne National Laboratory was funded by the Department of Energy, Office of Basic Energy Sciences, under Contract No. DE-AC02-06CH11357, which also funds

Argonne's Center for Nanoscale Materials (CNM) where the patterning of the BSCCO mesas was performed. We thank R Divan and L Ocola for their help with sample fabrication. GB thanks EPSRC, UK for financial support through Grant EP/I007210/1.

Appendix

As indicated by the temperature dependence of R_c below T_c as shown in figure 1 there are non-superconducting junctions which contribute a temperature dependent contact resistance that must be properly evaluated in order to reliably estimate the superconducting junction voltages. Figure A.1 shows the low-bias part of the I–V curves revealing that prior to the first superconducting switching a non-linear voltage signal arises due to these non-superconducting junctions which can be well described by $I = aV + bV^3$ [22]. With increasing temperature the I–V curves approach a linear characteristics; at 60 K a contact resistance of 3.3 Ω is obtained which is the value of R_c just below T_c. At low temperatures the low-bias limit of the non-linear I–V curves reproduces the R_c-values shown in figure 1. For the sake of a uniform presentation, in the inset of figure 1 the voltage values have been corrected for a contact resistance of 3.3 Ω. Since self-heating in the 'normal' region is negligible, we use the non-linear I–V curves prior to switching in the evaluation of the Josephson relation shown in figure 3(a). In the back-bending and forward-bending regions self-heating is predominant; therefore, as suggested by figure A.1(a) contact resistance of 3.3 Ω is appropriate. The high-bias data in figure 3(a) were obtained in this way.

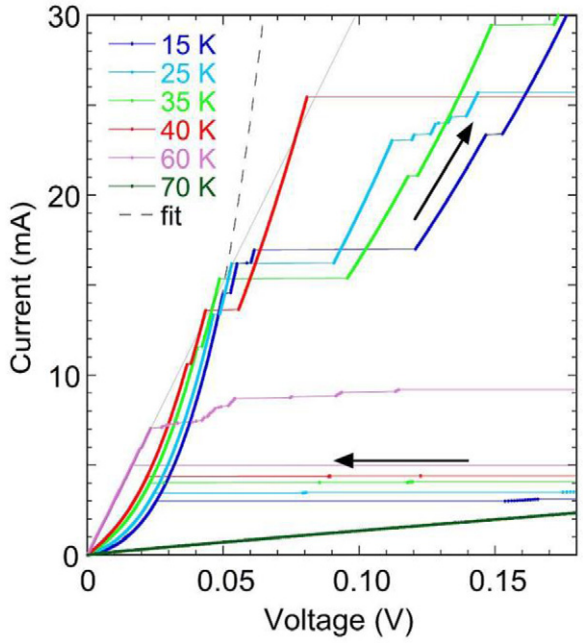

Figure A.1. Low-bias section of the I–V curves. Prior to the first superconducting switching a voltage signal appears that is well described as $I = aV + bV^3$ (dashed line) and which we attribute to non-superconducting junctions. At 60 K the I–V curve is linear, corresponding to a resistance of 3.3 Ω (solid line).

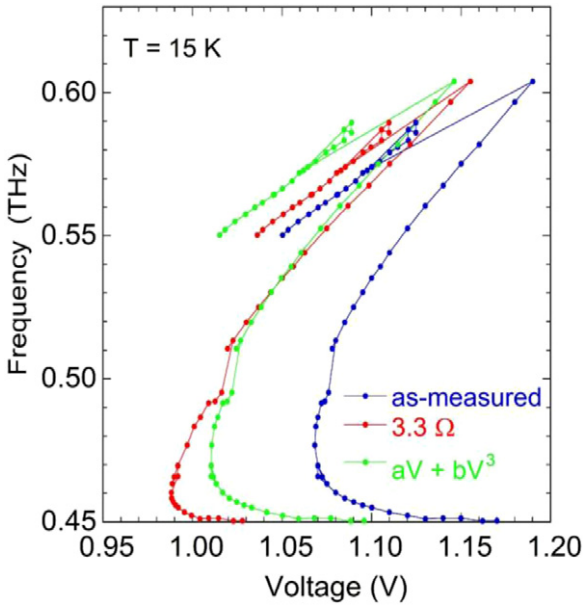

Figure A.2. Comparison of the effect of different treatments of the contact resistance on the frequency versus voltage diagram at 15 K.

As shown by the dashed and solid lines in figure A.1, there is some ambiguity in assigning the voltage values. However, this does not alter the conclusion of this work, namely that due to non-uniform temperature distributions along the c-axis the ac Josephson relation in terms of the applied mesa voltage does not hold. This can be seen from figure A.2, which shows for a temperature of 15 K the frequency versus voltage data as measured, with a uniform contact resistance of 3.3 Ω and a contact resistance given by the non-linear I–V prior to switching.

References

[1] Ozyuzer L *et al* 2007 *Science* **318** 1291
[2] Kleiner R, Steinmeyer F, Kunkel G and Mueller P 1992 *Phys. Rev. Lett.* **68** 2394
[3] Minami H, Kakeya I, Yamaguchi H, Yamamoto T and Kadowaki K 2009 *Appl. Phys. Lett.* **95** 232511
[4] Gray K E, Koshelev A E, Kurter C, Kadowaki K, Yamamoto T, Minami H, Yamaguchi H, Tachiki M, Kwok W-K and Welp U 2009 *IEEE Trans. Appl. Supercond.* **19** 886
[5] Wang H B, Guenon S, Yuan J, Iishi A, Arisawa S, Hatano T, Yamashita T, Koelle D and Kleiner R 2009 *Phys. Rev. Lett.* **102** 017006
[6] Tsujimoto M, Yamaki K, Deguchi K, Yamamoto T, Kashiwagi T, Minami H, Tachiki M, Kadowaki K and Klemm R A 2010 *Phys. Rev. Lett.* **105** 037005
[7] Guenon S *et al* 2010 *Phys. Rev.* B **82** 214506
[8] Kadowaki K, Tsujimoto M, Yamaki K, Yamamoto T, Kashiwagi T, Minami H, Tachiki M and Klemm R A 2010 *J. Phys. Soc. Japan* **79** 023703
[9] Wang H B *et al* 2010 *Phys. Rev. Lett.* **105** 057002
Yamaki K, Tsujimoto M, Yamamoto T, Furukawa A, Kashiwagi T, Minami H and Kadowaki K 2011 *Opt. Express* **19** 3193
[10] Benseman T M, Koshelev A E, Gray K E, Kwok W-K, Welp U, Kadowaki K, Tachiki M and Yamamoto T 2011 *Phys. Rev.* B **84** 064523
[11] Kashiwagi T *et al* 2012 *Japan. J. Appl. Phys.* **51** 010113

[12] Li M *et al* 2012 *Phys. Rev.* B **86** 060505
[13] Tsujimoto M, Yamamoto T, Delfanazari K, Nakayama R, Kitamura T, Sawamura M, Kashiwagi T, Minami H, Kadowaki K and Klemm R A 2012 *Phys. Rev. Lett.* **108** 107006
[14] Benseman T M, Koshelev A E, Kwok W-K, Welp U, Vlasko-Vlasov V K, Kadowaki K, Minami H and Watanabe C 2013 *J. Appl. Phys.* **113** 133902
[15] Koshelev A E 2008 *Phys. Rev.* B **78** 174509
[16] Kurter C *et al* 2009 *IEEE Appl. Supercond.* **19** 428
Kurter C *et al* 2010 *Phys. Rev.* B **81** 224518
Suzuki M *et al* 1999 *Phys. Rev. Lett.* **82** 5361
Wang H B *et al* 2005 *Appl. Phys. Lett.* **86** 023504
Fenton J C and Gough C E 2003 *J. Appl. Phys.* **94** 4665
Zavaritsky V N 2004 *Phys. Rev. Lett.* **92** 259701
Krasnov V M, Sandberg M and Zogaj I 2005 *Phys. Rev. Lett.* **94** 077003
[17] Minami H, Watanabe C, Sato K, Sekimoto S, Yamamoto T, Kashiwaki T, Klemm R A and Kadowaki K 2013 in preparation
[18] Yurgens A 2011 *Phys. Rev.* B **83** 184501
[19] Gross B *et al* 2012 *Phys. Rev.* B **86** 094524
[20] Balakrishnan G, Paul D M, Lees M R and Boothroyd A T 1993 *Physica* C **206** 148
Benseman T M 2007 *PhD Thesis* University of Cambridge
[21] Benseman T M, Cooper J R, Zentile C L, Lemberger L and Balakrishnan G 2011 *Phys. Rev.* B **84** 144503
[22] Takeya J, Akita S, Shimoyama J and Kishio K 1996 *Physica* C **261** 21
Yurgens A, Winkler D, Zavaritsky N V and Claeson T 1997 *Phys. Rev. Lett.* **79** 5122
Latyshev Yu I, Yamashita T, Bulaevskii L N, Graf M J, Balatsky A V and Maley M P 1999 *Phys. Rev. Lett.* **82** 5345
[23] Omukai Y, Kakeya I and Suzuki M 2012 *J. Phys.: Conf. Ser.* **400** 052027